

Prediction of glass forming ability in $\text{Cu}_x\text{Zr}_{1-x}$ alloys using molecular dynamics

M. M. Khandpekar^{1*}, A. Shrivastava¹, D. S. Gowtam², M. Mohape², V. P. Deshmukh²

¹Materials Research Lab, Department of Physics, Birla College,
Kalyan – 421304, India

²Naval Material Research Lab, Shil-Badlapur Road Ambernath,
Thane, Maharashtra – 42150, India

*dr_mmk1968@yahoo.com

PACS 61.43.Bn, 61.43.Dq, 61.43.Fs, 61.66.Dk DOI 10.17586/2220-8054-2015-6-5-650-660

Binary $\text{Cu}_x\text{Zr}_{1-x}$ ($x = 0.46, 0.50, 0.58, 0.62$) alloy systems were developed using a conventional melting route. Molecular dynamics (MD) simulations have been carried out using the embedded atom method (EAM) potentials. Radial distribution function (RDF) and Voronoi calculations have been conceded for amorphous structure verification. The reduced glass transition temperature (T_{rg}) has been determined in order to predict the glass forming ability (GFA) of these alloys. T_l is found to be a better substitute for T_m and the simulated T_{rg} values are seen to be in good agreement with the experimental results in limits of 0.8 – 5.4 %.

Keywords: Amorphous materials, Simulation and Modelling, Structural and thermal properties.

Received: 4 June 2015

Revised: 3 July 2015

Final revision: 15 September 2015

1. Introduction

The excellent properties of metallic glasses over their crystalline counterparts have attracted the attention of the scientific and industrial communities [1–4]. The challenge lies in predicting the glass forming compositions and thus, has been an active area of research [5–10]. Several empirical rules and criteria such as, an alloy must contain more than two elements, negative heat of mixing between the constituent atoms, low liquid eutectic, have been proposed to predict the glass forming ability (GFA) followed by rigorous experimentation [11–14]. Certainly, these rules have played an important role in providing enough information to synthesize bulk metallic glasses (BMGs), but experiments have also suggested that a minor change in composition can effectively change GFA [15].

Hence, it is essential to employ simulations and modeling methods for the prediction of GFA in order to reduce the associated time, energy and costs associated with these studies. Binary alloys are basically simple to model and as a result of the possibility of wide glass-forming compositions in Cu–Zr binary systems, they may be considered to be perfect systems for the prediction of GFA [16]. Additionally, Cu–Zr systems have experimental data availability (Table 1) [13, 14] for the comparison, and accessibility of EAM potentials for Cu and Zr elements for simulation.

One such simulation method which can be used to understand the behavior of metallic glasses at the atomic level and to predict GFA is Molecular dynamics (MD). In the present work, MD simulations have been applied to binary $\text{Cu}_x\text{Zr}_{1-x}$ alloys in order to predict their GFA. Reduced glass transition temperature criteria ($T_{rg} = T_g/T_l$ or T_g/T_m , where T_m is the

TABLE 1. EAM potential parameters [13, 14]

Elements	Structure	a (Å)	E_C (eV)	C_{11} (GPA)	C_{12} (GPA)	C_{44} (GPA)
Cu	fcc	3.6149 ^a	-3.5400	168.062	123.754	78.84
		3.61 ^b	3.49	168.4	121.4	75.4
Zr	hcp	3.230 ^c	-5.150	143.4	72.8	32
		3.232 ^d	-6.32	153	67	36

^{a,c} EAM, ^{b,d} Experiments

onset melting temperature T_g is the glass transition temperature, T_l is the liquidus temperature) have been employed in the GFA prediction process [14]. T_g and T_l are calculated using Wendt-Abraham (WA) parameter [17] and volume temperature ($V-T$) curve. The relationship between the melting temperature (obtained from the MD simulation) and experimental T_l values have been correlated and compared with those reported previously [18, 19].

2. Simulation and experimental methods

2.1. Simulation

To obtain an atomic description of the crystallization process and glass formation during rapid cooling of alloys, the MD simulation technique was adopted. The embedded atom method [20] (EAM)-based potential was used to represent the pair-wise atomic interaction between Cu and Zr atoms in the liquid and amorphous states.

The molecular dynamics simulation (MD) of the copper-zirconium alloy was carried out using constant number of particles-pressure-temperature (NPT) ensemble. To model the atomic interactions, EAM potentials provided with in Large-scale atomic/molecular massively parallel simulator software (LAMMPS) [21] was used to simulate the $\text{Cu}_x\text{Zr}_{1-x}$ ($x = 0.46, 0.50, 0.58, 0.62$) alloy systems. The simulated system consisted of 5000 atoms in a cubic unit cell of B2 structure with in periodic boundary conditions. The number of Cu atoms was replaced with number of Zr atoms according to the atomic percentage defined for the system under study. First, the model system was heated at 300 K to relax the system, then temperature was raised up to 3000 K and held there for 400 picoseconds (ps) in order to allow atoms to forget their initial structure. After that, the system was rapidly cooled to 2100 K and then slowly cooled from liquid state to 300 K at a cooling rate of 1×10^{11} K/s. At each temperature, the quantities of interest were obtained by taking averages over 80 ps. The MD time step selected for the simulation was 2 fs ($1 \text{ fs} = 1 \times 10^{-15}$ second). The Voronoi atomic clusters of each composition were analyzed at 600K using OVITO [22].

In order to check the size effect, a system of 10000 atoms was also utilized for calculation. The simulation shows very small finite size effect on the on the structural properties. A schematic approach has been displayed adopted in this work in Fig. 1.

2.2. Experiments

In order to validate the simulation results, experiments were also performed. To prepare the alloy ingots of the system studied in present work, first Cu and Zr ingots (Sigma-Aldrich, India) of purity percentage 99.99 % and 99.95 % respectively were ultrasonically cleaned; then, each ingot was melted in vacuum arc plasma melting furnace on a water cooled copper

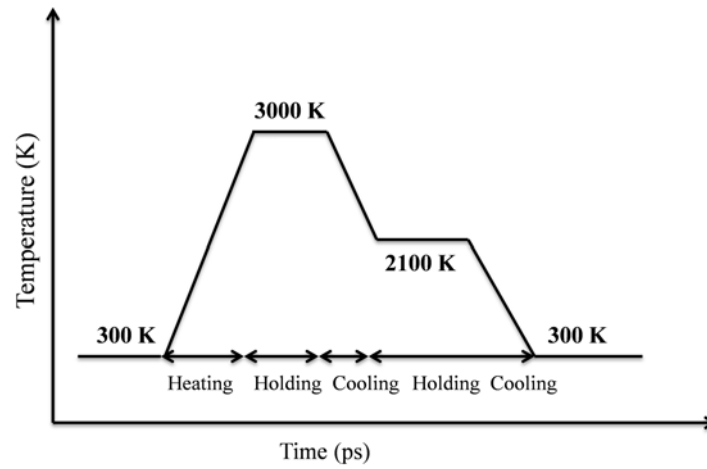


FIG. 1. Simulation schedule for studied alloy systems

plate under T_i gettered with a high purity argon atmosphere (6 bar). Each ingot was flipped over and remelted at least 4 – 5 times to obtain chemical homogeneity. The ingots were then melted again under high vacuum in glass test tube and casted in the form of amorphous ribbons using melt spinning. The prepared ribbons were then examined by a Panalytical 3040/60 X-ray diffractometer (XRD) using Cu- K_α source to investigate the present phase of the system. A differential scanning calorimeter (Hitachi DSC 6300) with heating rate of 20 °C/minute and argon atmosphere was used to confirm the amorphous structure by studying the glass transition temperature and crystallization temperature.

3. Results and discussion

3.1. Radial distribution function (RDF) and Voronoi tessellation

RDF is one of the most powerful techniques used for analyzing the inherent structure of liquids and amorphous alloys. It describes the spatial distribution of all other atoms with respect to the origin atom. For the bulk materials, it is given by:

$$G(r) = \frac{V}{N^2} \left\langle \sum_i \sum_{i \neq j} \delta(r - r_{ij}) \right\rangle, \quad (1)$$

where N is the number of atoms, V is volume of the cell, r and r_{ij} are the position of reference and other atoms, $G(r)$ is the probability of finding the atoms in the simulation box. For a random distribution, $G(r)$ always tends to unity. For a binary alloy system i.e. alloy containing at least atom 1 and atom 2, the radial distribution function (RDF) was calculated in the following manner:

$$G_{12}(r) = \frac{V}{N_1 N_2} \left\langle \sum_1 \sum_{1 \neq 2} \delta(r - r_{12}) \right\rangle. \quad (2)$$

Figures 2a and 2b represent the characteristic RDF's of pure copper and Zirconium at room temperature, at liquid state and in super cooled state. The sharp maxima observed in the RDF of pure copper and Zirconium at room temperature is found to correspond to the minimum bond length and crystalline state can be identified by sharp maxima. With an increase in

temperature, the height of first peak of $G(r)$ is found to decrease. The broadening in the second peak indicates that the model system is in a disordered or liquid state; though first nearest neighbors were almost equivalent to their crystalline counterpart. The difference however was observed in the lower and diffuse second peaks. Cooling of the melt rapidly down to 300 K, shows a slight increase in bond length which is attributable to the rearrangement of atoms. Due to this, the values of $G(r)_{\text{Cu-Cu}}$ and $G(r)_{\text{Zr-Zr}}$ are lower in super cooled state as compared to its ordered structure.

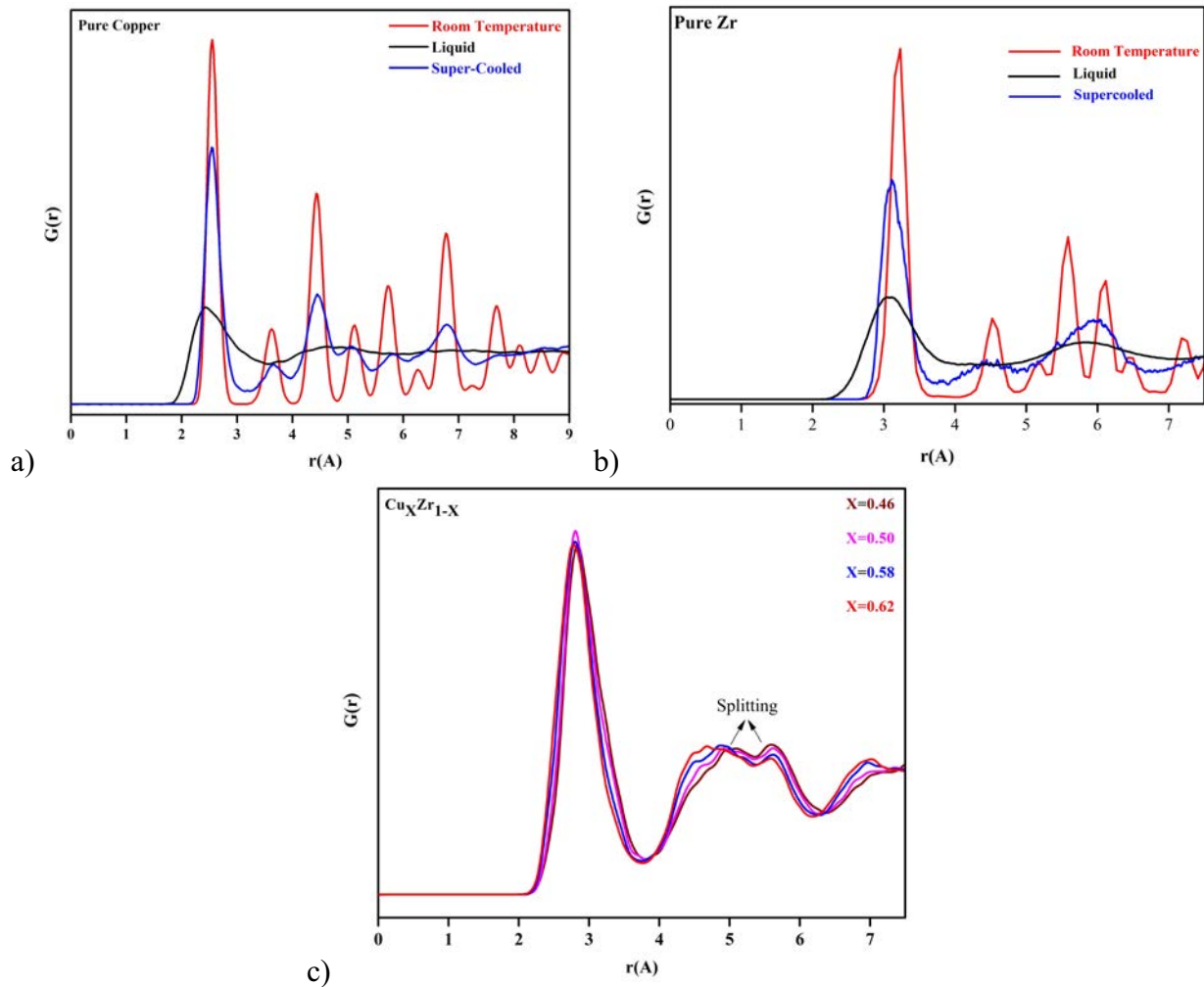


FIG. 2. RDF of Copper at (a) the room temperature, liquid state and super cooled state, Zirconium at (b) the room temperature, liquid state and super cooled state (c) $\text{Cu}_x\text{Zr}_{1-x}$ ($x = 0.46, 0.50, 0.58, 0.62$) in super cooled state

From Fig. 2c, it is clear that the addition of zirconium to copper shifts the first peak towards the higher 'r' values. This is due to the lower atomic radius of Cu (1.27 Å) as compared to that of Zr (1.60 Å). A splitting (marked) indicating characteristic of metallic glasses [23] is seen to make its presence in the second peak of the Copper alloy RDF plot. Further analysis of Fig. 2c showed that, upon super-cooling, there was no change in the height of the first peak, while second peak showed very slight variation. This led us to the conclusion that the super-cooled state is characterized by a local atomic arrangement to that of a liquid state.

To further analyze the local atomic arrangement, the Voronoi tessellation [24,25] method was employed. The Voronoi index is represented by a vector notation $\langle n_3, n_4, n_5, n_6 \rangle$ where n_i

denotes the number of shell atoms which are connected by other shell atoms defined by RDF. A cut off distance of 5 Å [26] was selected for Voronoi polyhedra (VP) calculation. The total fractions of various VP around Cu and Zr are shown in the Fig. 3 and Fig. 4.

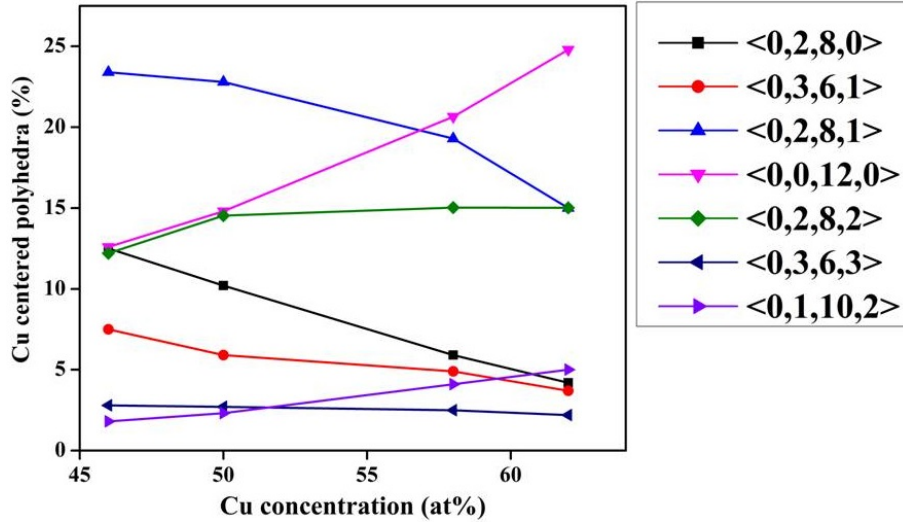


FIG. 3. Voronoi Fractions of around Cu in simulated Cu-Zr MGs at 600 K

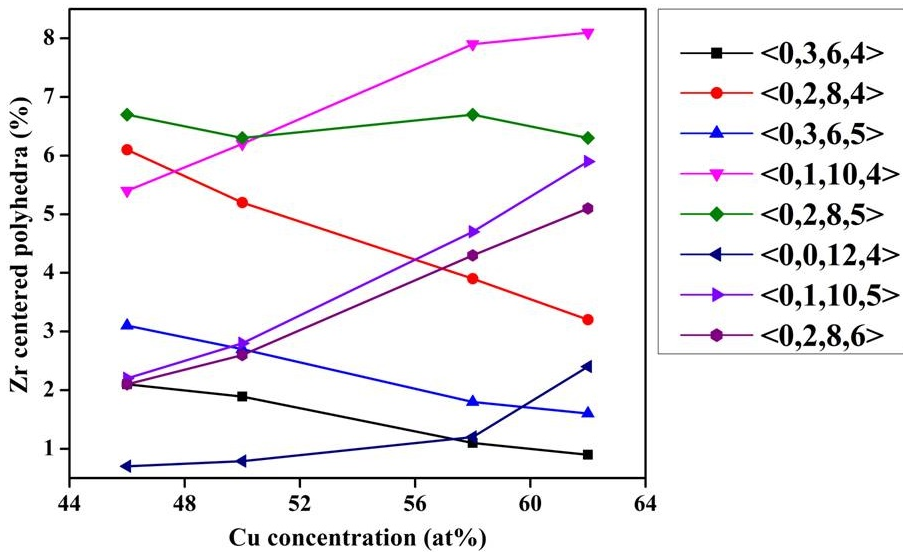


FIG. 4. Voronoi Fractions of around Zr in simulated Cu-Zr MGs at 600 K

From Fig. 3 it was observed, as concentration of Cu atoms increases from 46 at % (atomic percent) to 62 at %, the population of Cu centered five edges icosahedra face i.e., $\langle 0,0,12,0 \rangle$ and icosadihedra $\langle 0,1,0,12 \rangle$ increases, while the population of other polyhedra the such as $\langle 0,2,8,0 \rangle$, $\langle 0,2,8,1 \rangle$, $\langle 0,3,6,1 \rangle$ decreases, except to $\langle 0,2,8,2 \rangle$ which increases only to 50 at % and remains constant along with $\langle 0,3,6,3 \rangle$ polyhedra. This population variation of Cu center clusters was found to be consistent with the GFA of CuZr systems [27–29].

Some investigation of Zr centered VP clusters, shown in Fig. 4, suggested that the population of Zr polyhedra $\langle 0,1,10,4 \rangle$, $\langle 0,1,10,5 \rangle$, $\langle 0,2,8,6 \rangle$ and $\langle 0,0,12,4 \rangle$ gradually increased maximum up to 8 % , while the population of $\langle 0,2,8,4 \rangle$, $\langle 0,3,6,4 \rangle$, $\langle 0,3,6,5 \rangle$ lowered to 2 –

4 % and $\langle 0, 2, 8, 5 \rangle$ remained fairly constant at 7 %. This supports the hypothesis of Peng [24], which asserts that the population of these Zr centered clusters may fundamentally determine the dynamics in the CuZr system. The analysis of both Cu- and Zr- centered VP clusters implies that the Cu-centered $\langle 0, 0, 12, 0 \rangle$ VP enhances the stability of the system with Cu concentration, while other clusters slow the dynamics and both are responsible for amorphous structure evolution in the CuZr system.

The amorphous nature of our model system was experimentally confirmed by the XRD analysis of melt spun ribbons. Fig. 5 shows the XRD patterns of the melt spun ribbons of $\text{Cu}_x\text{Zr}_{1-x}$ ($x = 0.46, 0.50, 0.58, 0.62$). It can clearly be seen from the figure, that all exhibit broad diffraction maxima with no sign of the crystalline peak, thus confirming the amorphous nature.

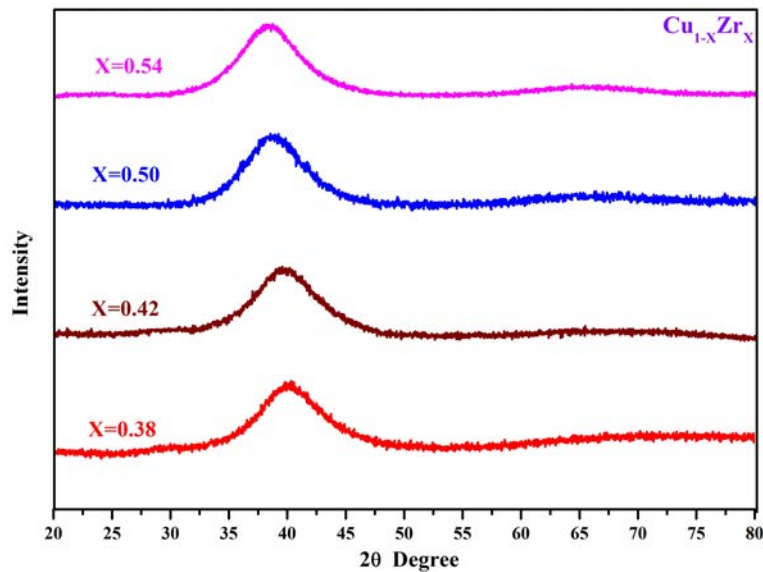


FIG. 5. X-ray diffraction pattern of melt spun ribbons of $\text{Cu}_x\text{Zr}_{1-x}$ ($x = 0.46, 0.50, 0.58, 0.62$)

3.2. Melting and Glass Transition temperatures

To further explain the melting and glass transition in amorphous Cu–Zr system, volume temperature ($V - T$) curves were calculated during heating and cooling (not shown in figure). Fig. 6 displays the change in volume as a function of temperature for simulated alloy systems. As the temperature of the model system is raised from 300 to 3000 K at a constant heating rate, the volume is found to increase linearly. A sudden jump in the $V - T$ curves occurs, indicating a rapid increase in volume. This sudden jump is an indication of a phase transformation; i.e. it corresponds to the melting (T_i) of the system.

A parameter known as the Wendt-Abraham (WA) parameter ($R_{WA} = G_{\min}/G_{\max}$), often used as a measure of glass transition, was used to determine T_g of the system under study. G_{\min} represents the value of $G(r)$ at the first minimum and G_{\max} the value of $G(r)$ at the first maximum in the RDF curve. Fig. 7 shows a plot between RWA against temperature. The point of intersection was determined and adopted as T_g . The WA parameter provides direct comparison to structures since it emphasizes the local character of $G(r)$, leading to better estimation of the glass transition temperature. It is well known, that the glass transition temperature is not a true second order phase transition, since it is dependent on the cooling rates. Faster cooling rate results the higher glass transition temperature due to less time available for

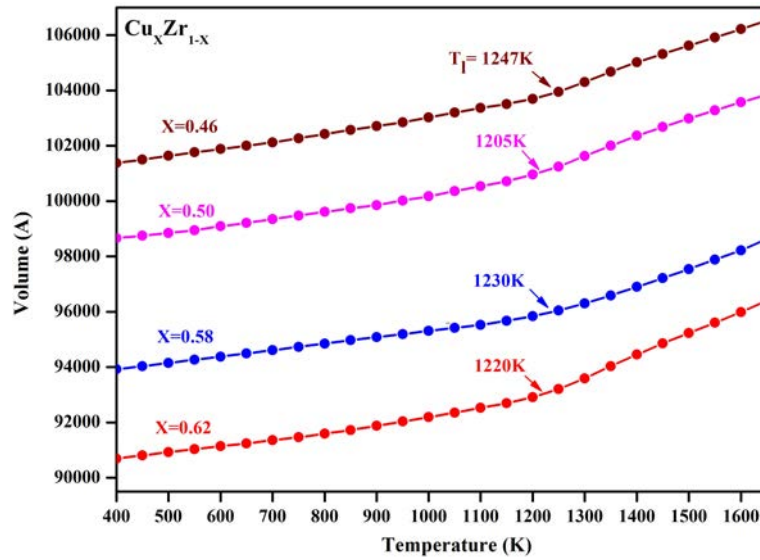


FIG. 6. Variation in cell volume with temperature for $\text{Cu}_x\text{Zr}_{1-x}$

atoms to relax. Around T_g , a change in volume, enthalpy and entropy are continuous, but their derivatives such as heat capacity and thermal expansion coefficient are discontinuous. With the chosen cooling rates in present work, the calculated T_g was found to be close to the laboratory-determined experimental values and the simulated T_g was believed to be reliable for Cu–Zr system. Furthermore, Duan et al. [30] have used tight binding potentials to simulate T_g for $\text{Cu}_{0.46}\text{Zr}_{0.54}$, and Su-Wen Kao et al. [17], using the same potentials, have also calculated T_g for $\text{Cu}_x\text{Zr}_{100-x}$ ($x = 46, 50, 62$) and found that these values are similar to those determined experimentally (i.e. differs by 2 – 8 %).

The DSC curves of the synthesized alloy systems are depicted in Fig. 8. A strip of sample amorphous ribbon was heated at a constant rate. The DSC curve shows a clear endothermic peak, which is characteristic of a glass transition temperature (T_g) followed by an exothermic crystallization peak. The other deep endothermic peak, of which starting point is solidus melting temperature (T_m) and end point is liquidus temperature (T_l), were associated with the simulated melting. The deviation in the T_g , and T_l obtained from MD and experimental values are found to lie between 1.3 – 6.2 %, and 1 – 2.5 % respectively. Despite the very high heating and cooling rate, the precision between the simulated and experimental value implies that a viscosity change from solid to super cooled liquid is not a second order phase transition and involves no latent heat of transition, thus further confirming the accuracy of simulation against the experimentation.

3.3. Reduced glass transition temperature

When a liquid alloy is cooled from the molten state down to a temperature below T_g , the viscosity of the melt increases to a high value and a glass is formed. Based on nucleation kinetics viscosity calculation, Turnbull [15] have mentioned, an alloy with high value of T_g and low value of T_l would easily form a glass. This ratio has been designated as reduced glass transition temperature (T_{rg}). The higher the T_{rg} value, the higher the viscosity of melt is and it is more easily solidified into a glassy state at a lower cooling rate.

Table 2 shows simulated and experimental T_g , T_m , T_l , and T_{rg} for $\text{Cu}_x\text{Zr}_{1-x}$ ($x = 0.46, 0.50, 0.58, 0.62$) alloys. It was rather difficult to distinguish between T_m and T_l , as the $V - T$ plot (generated by MD simulation) indicated a single shift for the melting in

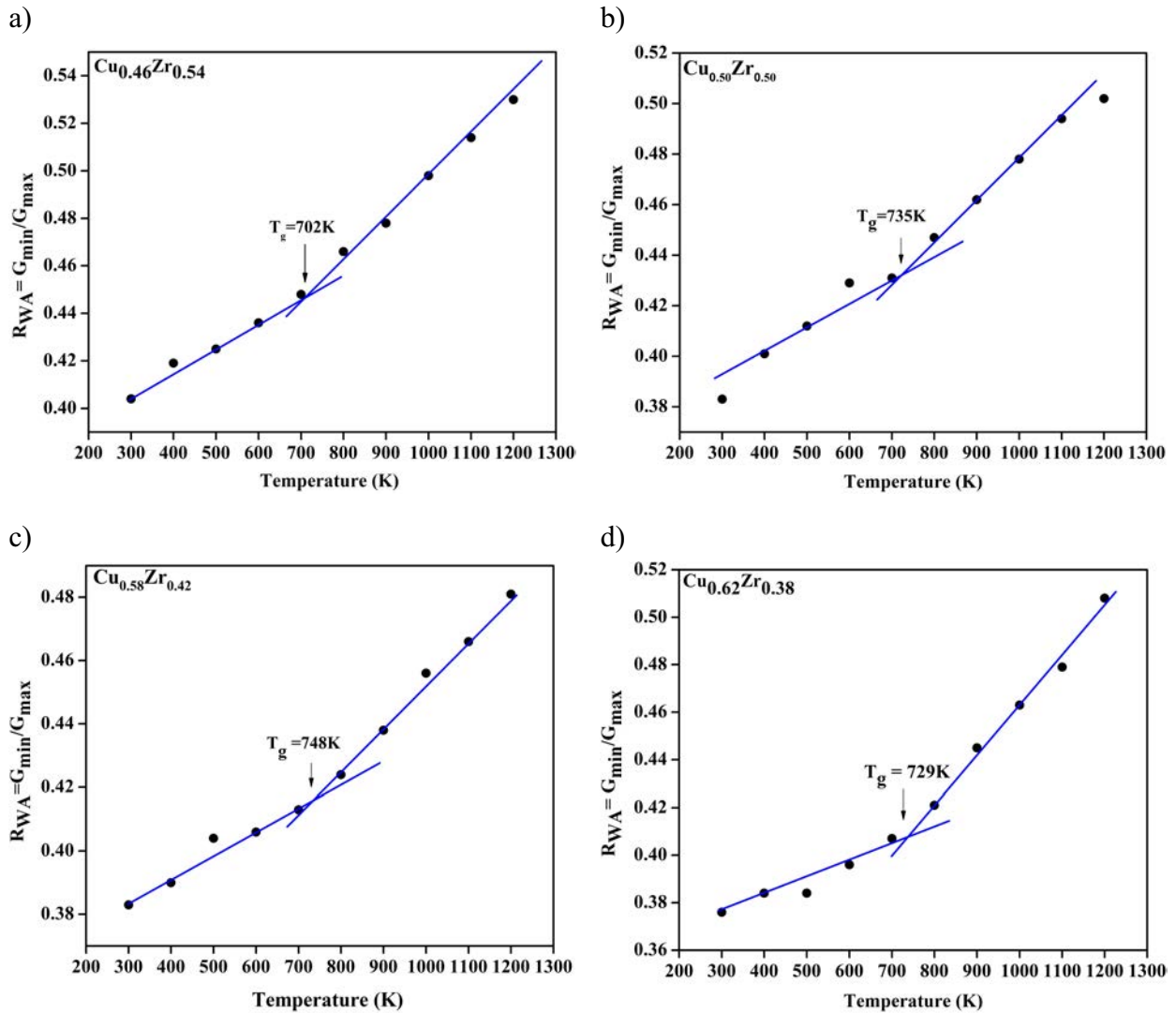
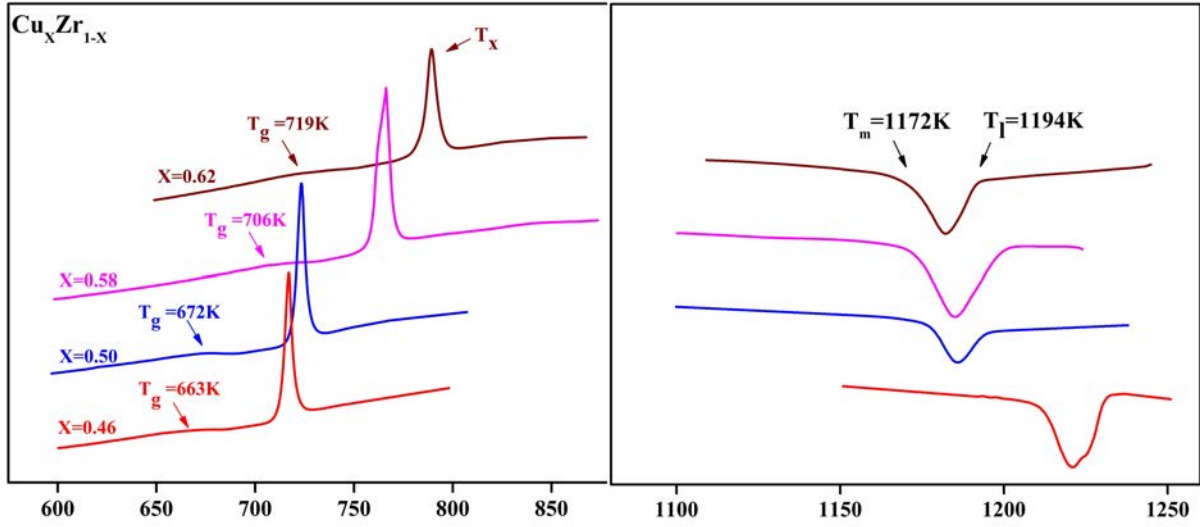


FIG. 7. Wendt Abraham (RWA) parameter as a function of temperature for $\text{Cu}_{0.46}\text{Zr}_{0.54}$

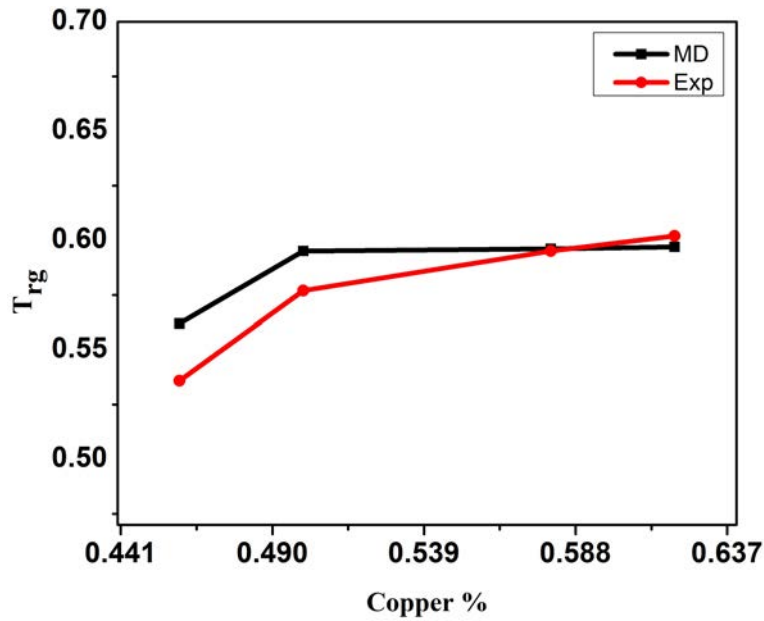
Cu–Zr alloy system. Additionally, the simulated melting temperature values were found to lie closer to experimental T_l values rather than T_m . Hence, the T_{rg} values were calculated using T_g/T_l as emphasized by Turnbull instead of the T_g/T_m ratio. Simulated T_{rg} values are well found to be in good agreement with experimental values with deviation lying between 0.8 – 5.4 %. These results further support our assumption that T_l is a better substitute for T_m . That is, when calculating T_{rg} from MD, for a Cu–Zr binary alloy, one should avoid the interchange of T_m to T_l and melting temperature (obtained from MD) should be considered as the liquidus temperature instead of solidus temperature. It is also clear from the Fig. 9 that T_{rg} obtained from the simulation and experiments follow the same trend against the copper content, which confirms the consistency between the theoretical and experimental results.

4. Conclusion

The relationship between GFA and T_{rg} for $\text{Cu}_x\text{Zr}_{1-x}$ ($x = 0.46, 0.50, 0.58, 0.62$) alloys has been studied by MD simulations. The amorphous structure of the alloy system was confirmed by RDF and Voronoi calculation. It was found that the population of Cu centered Voronoi

FIG. 8. DSC scan of melt spin ribbons of $\text{Cu}_x\text{Zr}_{1-x}$ TABLE 2. The simulated and calculated T_l , T_g and T_{rg} values for $\text{Cu}_x\text{Zr}_{1-x}$ alloys

Compositions	MD (K)			Experiments (K)			
	T_l	T_g	T_{rg}	T_m	T_l	T_g	T_{rg}
$\text{Cu}_{0.46}\text{Zr}_{0.54}$	1247	702	0.562	1209	1232	663	0.538
$\text{Cu}_{0.50}\text{Zr}_{0.50}$	1205	717	0.595	1178	1193	672	0.563
$\text{Cu}_{0.58}\text{Zr}_{0.42}$	1230	733	0.596	1173	1199	706	0.588
$\text{Cu}_{0.62}\text{Zr}_{0.38}$	1220	729	0.597	1172	1194	719	0.602

FIG. 9. Experimental versus Simulated T_{rg} of $\text{Cu}_x\text{Zr}_{1-x}$

polyhedra $\langle 0, 0, 12, 0 \rangle$ increases the amorphous phase stability, with Cu content. Experiments were carried out in order to validate the accuracy of the simulated quantities. The difference between the experimental and simulated T_l , T_g and T_{rg} values lies within the accuracy limit of 1.3 – 6.2 %, 1 – 2.5 % and 0.8 – 5.4 % respectively, better than those reported [6]. Nearly same trend has been attained in simulated and experimental T_{rg} values. Thus MD simulation offers a reliable way to predict the GFA of alloys systems whose constituent elements have well defined EAM potentials.

Acknowledgments

The authors are grateful to Dr. R. S. Hastak, Director NMRL, for his research support, Dr. B. C. Chakraborty, Dr. G. Gunasekaran, Dr. S. Rath of NMRL, M. Bharadwaj of CSTEP, Bangalore and Dr. S. Subramanian, DMRL, Hyderabad for their useful discussions.

References

- [1] Guo F.Q., Poon S.J., Shiflet G. J. CaAl-based bulk metallic glasses with high thermal stability. *Appl. Phys. Lett.*, 2004, **84**, P. 37–39.
- [2] Fan C., Takeuchi A., Inoue A. Preparation and mechanical properties of Zr-based bulk nanocrystalline alloys containing compound and amorphous phases. *Mater. Trans. JIM*, 1999, **40**, P. 42–51.
- [3] Drehman A.J., Greer A.L., Turnbull D. Bulk formation of a metallic glass: palladium-nickel-phosphorus ($\text{Pd}_{40}\text{Ni}_{40}\text{P}_{20}$). *Appl. Phys. Lett.*, 1982, **41**, P. 716.
- [4] Inoue A., Zhang T., Masumoto T. Production of amorphous cylinder and sheet of $\text{La}_{55}\text{Al}_{25}\text{Ni}_{20}$ alloy by metallic mould casting method. *Mater. Trans. JIM*, 1990, **31**, P. 425–428.
- [5] Pecker A., Johnson W.L. A highly processable metallic glass: $\text{Zr}_{41.2}\text{Ti}_{13.8}\text{Cu}_{12.5}\text{Ni}_{10.0}\text{Be}_{22.5}$. *Appl. Phys. Lett.*, 1993, **63**, P. 2342–2344.
- [6] Zhang T., Inoue. A, Masumoto T. Amorphous Zr–Al–Tm (Tm=Co, Ni, Cu) alloys with significant supercooled liquid region of over 100 K. *Mater Trans. JIM*, 1991, **32**, P. 1005–1010.
- [7] Johnson W.L. Bulk glass-forming metallic alloys: science and technology. *Mater. Res. Bull.*, 1999, **24**, P. 42–56.
- [8] Loffler J.F. Bulk metallic glasses. *Intermetallics*, 2003, **11**, P. 529–540.
- [9] Lu Z.P., Liu. C.T. Glass formation criterion for various glass-forming systems. *Phys. Rev. Lett.*, 2003, **91**, P. 115505.
- [10] Inoue A. Stabilization of metallic supercooled liquid and bulk amorphous alloys. *Acta Mater.*, 2000, **48**, P. 279–306.
- [11] Inoue A., Zhang T., Masumoto T. Glass-forming ability of alloys. *J. Non-Cryst. Solids.*, 1993, **156**, P. 473–480.
- [12] Cheng Y.Q., Sheng H.W., Ma E. Relationship between structure, dynamics, and mechanical properties in metallic glass-forming alloys. *Phys. Rev. B*, 2008, **78**, P. 014207.
- [13] Li Y., Poon S.J., et al. Formation of bulk metallic glasses and their composites. *MRS Bull.*, 2007, **32**, P. 624–628.
- [14] Kittel C. *Introduction to Solid State Physics*. Wiley, New York, 2005, 704 p.
- [15] Cohen E.R., Lide D.R., Trigg G.L. *AIP Physics Desk Reference*. AIP Press, New York, 2003, 843 p.
- [16] Turnbull D. Under What Conditions can a Glass be Formed? *Cont. Phys.*, 1969, **10** (5), P. 473–488.
- [17] Wendt H.R., Abraham F.F. Empirical Criterion for the Glass Transition Region Based on Monte Carlo Simulations. *Phys. Rev. Lett.*, 1978, **41**, P. 1244.
- [18] Kao S.W., Hwang C.C., Chi T.S. Simulation of reduced glass transition temperature of Cu–Zr alloys by molecular dynamics. *J. Appl. Phys.*, 2009, **105**, P. 064913.
- [19] Gunawardana K.G.S.H., Wilson S.R., Mendelev M.I., Song X. Theoretical calculation of the melting curve of Cu–Zr binary alloys. *Phys. Rev. E*, 2014, **90**, P. 052403.
- [20] Mendelev M.I., Sordelet D.J., Kramer M.J. Using atomistic computer simulations to analyze X-ray diffraction data from metallic glasses. *J. Appl. Phys.*, 2007, **102**, P. 043501.
- [21] Plimpton S.J. Fast parallel algorithms for short-range molecular dynamics. *Comp. Phys.*, 1995, **117**, P. 1–19.
- [22] Stukowski A. Visualization and analysis of atomistic simulation data with OVITO – the Open Visualization Tool. *Mater. Sci. Eng.*, 2010, **18**, P. 015012.

- [23] Qi Y., Cagin T., Kimura Y., Goddard W.A. Molecular-Dynamics Simulations of Glass Forming and Crystallization in Binary Liquid Metals: Cu–Ag and Cu–Ni. *Phys. Rev. B*, 1999, **59**, P. 3527–3533.
- [24] Finney J.L. Modelling the structures of amorphous metals and alloys. *Nature*, 1977, **266**, P. 309–314.
- [25] Stepanyuk V.S., Katsnelson A.A., et al. Microstructure and its relaxation in FeB amorphous system simulated by molecular dynamics. *J. Non-Cryst. Solids.*, 1993, **159**, P. 80–87.
- [26] Peng H.L., Li M.Z., et al. Effect of local structures and atomic packing on glass forming ability in $\text{Cu}_x\text{Zr}_{100-x}$ metallic glasses. *Appl. Phys. Lett.*, 2010, **96**, P. 021901.
- [27] Tang M.B., Zhao D.Q., Pan M.X., Wang W.H. Binary Cu–Zr bulk metallic glasses. *Chin. Phys. Lett.*, 2004, **21**, P. 901–903.
- [28] Park K.W., Jang J.I., et al. Atomic packing density and its influence on the properties of Cu–Zr amorphous alloys. *Scr. Mater.*, 2007, **57**, P. 805–808.
- [29] Ma D., Stoica A.D., et al. Efficient local atomic packing in metallic glasses and its correlation with glass-forming ability. *Phys. Rev. B*, 2009, **80**, P. 014202.
- [30] Duan G., Xu D., et al. Molecular dynamics study of the binary $\text{Cu}_{46}\text{Zr}_{54}$ metallic glass motivated by experiments: Glass formation and atomic-level structure. *Phys. Rev. B*, 2005, **71**, P. 224208.